BIOCHEMISTRY
including biophysical chemistry & molecular biology
Article

Biochemistry **2010,** *49,* 945–950 945
DOI: 10.1021/bi901594w

Molecular Mechanisms Underlying the Early Stage of Protein Translocation through the Sec Translocon†

Takaharu Mori,‡,§ Ryuichiro Ishitani,∥ Tomoya Tsukazaki,∥ Osamu Nureki,∥ and Yuji Sugita*,‡,§,⊥

‡*RIKEN Advanced Science Institute, 2-1 Hirosawa, Wako-shi, Saitama 351-0198, Japan,* §*BIRD, JST, 2-1 Hirosawa, Wako-shi, Saitama 351-0198, Japan,* ∥*Division of Structure Biology, Department of Basic Medical Science, Institute of Medical Science, University of Tokyo, 4-6-1 Shiroganedai, Minato-ku, Tokyo 108-8639, Japan, and* ⊥*CREST, JST, 2-1 Hirosawa, Wako-shi, Saitama 351-0198, Japan*

Received September 11, 2009; Revised Manuscript Received December 28, 2009

ABSTRACT: The Sec translocon, a protein-conducting channel, consists of a heterotrimeric complex (SecYEG in bacteria and Sec61$\alpha\beta\gamma$ in eukaryotes) that provides a pathway for secretary proteins to cross membranes, or for membrane proteins to integrate into the membrane. The Sec translocon alone is a passive channel, and association with channel partners, including the ribosome or SecA ATPase in bacteria, is needed for protein translocation. Three recently published crystal structures of SecY are considered to represent the closed (resting state), pre-open (transitional state determined with the bound Fab fragment mimicking SecA interaction), and SecA-bound forms. To elucidate mechanisms of transition between closed and pre-open forms, we performed all-atom molecular dynamics simulations for the pre-open form of *Thermus thermophilus* SecYE and the closed form of *Methanococcus janaschii* SecYEβ in explicit solvent and membranes. We found that the closed form of SecY is stable, while the pre-open form without the Fab fragment undergoes large conformational changes toward the closed form. The pre-open form of SecY with Fab remains unchanged, suggesting that the cytosolic interaction mimicking SecA binding stabilizes the pre-open form of SecY. Importantly, a lipid molecule at the lateral gate region appears to be required to maintain the pre-open form in the membrane. We propose that the conformational transition from closed to pre-open states of SecY upon association with SecA facilitates intercalation of phospholipids at the lateral gate, inducing initial entry of the positively charged signal peptide into the channel.

Cellular secretion releases metabolites and macromolecules from the cell and is controlled by hormones, metabolic products, and enzymes. More than 30% of cell proteins are secreted across membranes or integrated into membranes. The Sec translocon plays a central role in these protein translocations (*1*, *2*). It consists of an evolutionarily conserved heterotrimeric membrane-protein complex, SecYEG in bacteria and Sec61$\alpha\beta\gamma$ in eukaryotes. SecY contains 10 transmembrane helices and provides a channel-like pathway for protein translocation. The SecY translocon alone is a passive channel, and the driving force for protein translocation is provided by channel partners, including the ribosome and SecA ATPase in bacteria (*3*−*8*). The association with channel partners induces pore opening and protein translocation through SecY. Biochemical approaches (*9*−*11*), X-ray crystallography (*1*, *12*−*14*), and molecular dynamics (MD)[1] simulations (*15*−*17*) have contributed to our understanding of the protein interactions, structure, and dynamics.

To date, three distinct structures of the SecY complex have been reported. The first was a "closed" form of *Methanococcus jannaschii* SecYEβ (mjSecYEβ) at 3.2 Å resolution (*1*). Here, SecY has two linked halves, TM1−5 and TM6−10, clamped together by SecE to form an hourglass-shaped pore. This form is characterized by three important structural features: (i) the lateral gate that is completely closed, (ii) the channel pore that is sealed by a pore ring on the cytoplasmic side, and (iii) the pore that is blocked by a short "plug" helix on the periplasmic side. The opening of the SecY channel would presumably involve lateral gating motions toward the lipid bilayer and vertical movements of the plug helix (*1*, *18*). More recently, two new crystal structures of the SecY complex were reported. One is the "SecA-bound" form of the *Thermotoga maritima* SecA−SecYEG complex (tmSecA−tmSecYEG) at 4.5 Å resolution (*13*). This structure contains one molecule of tmSecA bound to one copy of tmSecYEG, where the plug helix has moved from the center of the channel toward the periplasmic side. In addition, the "window" is wide open at the lateral gate region. The other crystal structure is a complex of *Thermus thermophilus* SecYE with the antibody Fab fragment at 3.2 Å resolution (Fab−ttSecYE) (*14*). This structure contains a hydrophobic "crack" open to the cytosol at the lateral gate, while the channel pore is closed with the plug helix and the pore ring. This conformation of ttSecY has been considered as a "pre-open" form in the translocation cycle, because (i) cross-linking experiments demonstrate that Fab and ttSecA bind to the identical region of ttSecY, (ii) the pattern of disulfide bond formation under the SecA-bound condition is different from that

†This work was supported in part by BIRD & CREST, Japan Science and Technology Agency (JST) (to Y.S.) and by a Grant for Scientific Research on Priority Area 'Membrane Interface' (to Y.S. and R.I.) and the Development and Use of the Next-Generation Supercomputer Project of the Ministry of Education, Culture, Sports, Science and Technology (MEXT) (to Y.S.).

*To whom correspondence should be addressed: RIKEN Advanced Science Institute, 2-1 Hirosawa, Wako-shi, Saitama 351-0198, Japan. Phone: +81-48-462-1407. Fax: +81-48-467-4532. E-mail: sugita@riken.jp.

[1]Abbreviations: MD, molecular dynamics; TM, transmembrane; PDB, Protein Data Bank; POPC, 1-palmitoyl-2-oleoyl-*sn*-glycero-3-phosphocholine; rmsd, root-mean-square deviation.

Published on Web 01/07/2010

without SecA or Fab, and (iii) a MD simulation of the Fab-free ttSecYE shows a conformational change toward the closed form (*14*). However, several questions still remain unsolved: what is the meaning of the hydrophobic crack in relation to the conformational changes between the closed and pre-open forms, and how does the binding of SecA or Fab induce the conformational change in the transmembrane region of SecY?

In this study, we performed all-atom MD simulations of Fab-free ttSecYE, the Fab−ttSecYE complex, and mjSecYEβ in the membrane to answer these questions. Significantly, we observed a strong correlation between the conformational changes in ttSecYE and the sideways movement of a phospholipid molecule in the lateral gate region. On the basis of the crystal structures and the current MD simulations, we propose novel molecular mechanisms for the early stage of translocation of protein through the Sec channel.

METHODS

We performed four MD simulations (Sim1−4) listed in Table S1 of the Supporting Information. Each starting conformation is shown in Figure S1 of the Supporting Information. The initial structure used in each simulation is the pre-open form of Fab-free ttSecYE (Sim1), the closed form of mjSecYEβ (Sim2), and the pre-open form of ttSecYE with Fab (Sim3 and Sim4). In Sim3, Fab was permitted to move freely, whereas in Sim4, Fab and the α-helix portion encompassing Lys43−Thr50 of ttSecY, which exhibit intermolecular contact in the crystal (*14*), were weakly restrained to reduce the movement of Fab and to investigate such an effect on the conformational change of ttSecYE in the membrane.

All-atom MD simulations were carried out using NAMD2 and the CHARMM27 force-field parameters with ϕ, ψ cross-term map correction (CMAP) (*19*−*21*). The X-ray structures (PDB entry 2ZJS without Fab for Sim1, 1RH5 for Sim2, and 2ZJS for Sim3 and Sim4) were embedded in equilibrated POPC bilayers in 150 mM NaCl. The details of the modeling procedure for the initial structures of the simulations are described in the Supporting Information. The systems were subjected to short energy minimizations to remove steric clashes in the initial structure, followed by short MD simulations for the equilibration with a gradual decrease in harmonic restraints on the heavy atoms in the protein (for detailed procedures, see the text of the Supporting Information); 100 ns MD simulations were then carried out in the NPT ensemble for the production dynamics in Sim1−4. In these simulations, constant pressure (1 atm) and constant temperature (300 K) were maintained using Langevin dynamics and Langevin piston, respectively. The particle mesh Ewald (PME) method was employed for the calculation of the electrostatic interactions (*22*). The equation of motion was integrated with a time step of 2 fs. Protein solvent accessibility, pore inside the protein, and domain motions in proteins were analyzed using NACCESS (*23*), MOLE (*24*), and DynDom (*25*), respectively. In this study, we also performed MD simulations of the same system for Sim1−4 in the NPAT ensemble, and the results were essentially the same as those in NPT (data not shown).

RESULTS AND DISCUSSION

Summary of the MD Simulations. In Sim1, a structural change near the lateral gate region is observed, while it is suppressed in Sim3 and Sim4 (Movies 1, 3, and 4 of the Supporting Information). In Sim2, the conformation of SecY

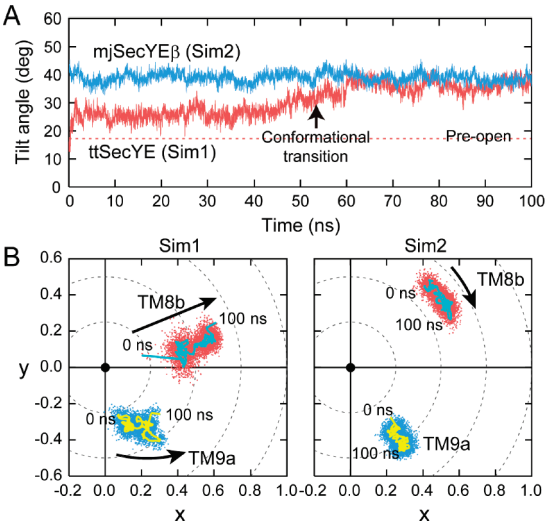

FIGURE 1: Time evolution of the orientation change of TM8b and TM9a in Sim1 and Sim2. TM8b and TM9a make up the C-terminal half of TM8 (Ile320−Val329 in ttSecY and Cys327−Thr338 in mjSecY) and the N-terminal half of TM9 (Thr368−Pro382 in ttSecY and Leu377−Leu388 in mjSecY), respectively. (A) Time course for the tilt angle of TM8b in Sim1 and Sim2. (B) Plots of the projection of the unit vectors of TM8b and TM9a onto the $X-Y$ plane (parallel to the membrane) in Sim1 (left) and Sim2 (right). Cyan and yellow lines represent the average trajectory of each helix movement, and the black circles represent the origin of each helix vector.

remains unchanged (Movie 2 of the Supporting Information). In all the simulations, SecE shows no conformational change. We observe small rmsd changes (<1.5 Å) in the transmembrane region of SecY with respect to the initial structures in all the simulations, implying successful equilibration for our simulation systems (text and Figure S2 of the Supporting Information). In all the simulations, we never observed positional and structural changes for the plug helix and pore ring (rmsd is <1.5 Å for the plug helix and <1.0 Å for the pore ring). Therefore, no hole at the center of the channel is created in the simulations (Figure S3 of the Supporting Information). We further calculate the minimum and average distances between the Cα atoms in residue pairs of SecY to examine whether the simulated structures of SecY are in keeping with the disulfide bond cross-linking experiments. We judged that a disulfide bond is able to form when the distance between the two Cα atoms of these residues is approximately ≤7 Å and found that the SecY structures in our simulations are consistent with the experiments (text, Table S2, and Figures S4 and S5 of the Supporting Information). Thus, SecY after the structural change in Sim1 is satisfied with three important structural features in the closed form as well as the experimental distance restraints. On the basis of these results, we judged that SecY undergoes a conformational change toward the closed form in Sim1, while SecY with Fab remain in pre-open forms in Sim3 and Sim4.

Dynamic Properties of the Pre-Open and Closed Forms. To examine the conformational changes of SecY in detail, we calculated the tilt angles of the TM helices in Sim1 (Fab-free ttSecYE) and compared them with those of Sim2 (mjSecYEβ). In calculating the tilt angles, we fitted the Cα atoms in all TM helices to the initial structure, allowing only the rigid-body translations and rotation in an $X-Y$ (membrane) plane to decouple the movement of the selected helix and entire protein structure. With the exception of TM8 and TM9, we did not observe any significant movements of the TM helices in Sim1. In Figure 1A,

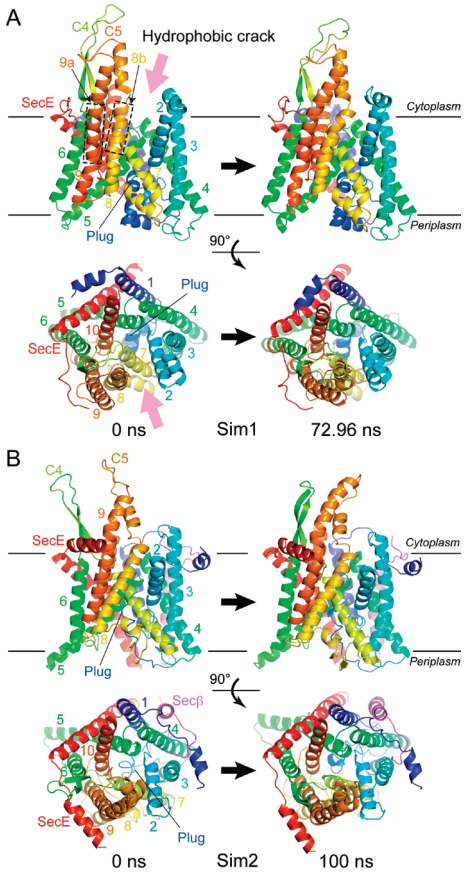

FIGURE 2: Snapshots of the MD trajectory in Sim1 and Sim2. (A) Initial (at 0 ns) and most closed structure (at 72.96 ns) of Fab-free ttSecYE in Sim1. (B) Initial (at 0 ns) and final structure (at 100 ns) of mjSecYEβ in Sim2.

TM8b (the C-terminal half of TM8) in Sim1 increases its tilt angle after 50 ns toward the value observed in Sim2, which remains constant over 100 ns. Thus, in Sim1, the conformation of SecY changes to the closed form (Figure 2A). Although the tilt angle of TM9a (the N-terminal half of TM9) does not change in Sim1, this portion of the helix rotates ~27° in an counterclockwise direction around an axis parallel to the bilayer normal (Figure 1B). As a result, the hydrophobic crack becomes filled by tilting of TM8 toward TM2 and rotation of TM9 toward TM8. The solvent accessible surface area of highly conserved amino acid residues in the crack, namely, Ile85, Pro273, Phe276, Ala277, and Tyr326, decreases by 49.3 Å^2 in the most closed structure at 72.96 ns (Figure 2A), where the distance between Thr92(TM2) and Val329(TM8) becomes the shortest during the run of 100 ns (Figures S4 and S5 of the Supporting Information).

In contrast, the conformational fluctuations of SecY in Sim2 are smaller than those observed in Sim1. As shown in Figure 2B, the final structure of Sim2 is virtually identical to the initial structure with the exception of the C4 and C5 loops. The tilt angles of TM8b and TM9a are almost unchanged over 100 ns, whereas TM8b rotates slightly in a clockwise direction around the axis parallel to the bilayer normal (Figure 1B). From these simulations, we suggest that the closed form of SecY is stable in the membrane, whereas the pre-open form without channel partners undergoes a conformational transition to the closed form.

Interaction between SecY and the Channel Partner. In Sim3, Fab itself shows significant flexibility, while SecY remains stable (Figure 3A). We detected a 21° rotation of the Fab itself around an axis almost parallel to the bilayer normal and an 18° bending motion of the upper half of the Fab around the axis closely parallel to the bilayer (Figure S6A of the Supporting Information). The rmsd of Fab fluctuates around 3.0 Å (Figure S6B of the Supporting Information). Despite such large motions of Fab in Sim3, TM8b and TM9 are observed to tilt only slightly toward TM2 (Figure 3A and Figure S7 of the Supporting Information), which consequently decreases the solvent accessible surface area of the hydrophobic crack by approximately 28.6 Å^2 in the final conformation of Sim3. The changes are significantly smaller than those in Sim1 (Fab-free ttSecYE). In Sim4, the movements of TM8b and TM9a are suppressed and the hydrophobic crack remains intact over 100 ns (Figure 3B and Figure S7 of the Supporting Information). These results suggest that the conformational flexibility of SecY is determined by the movements of Fab.

The epitope recognition site in Fab makes intensive interactions with Arg351 in ttSecY, which is located in the highly conserved motif sequence, ^{348}PGIRPG^{353}, in the C5 loop (*14*). Arg351 is an indispensable residue for channel activity (*26*−*28*), because both the ribosome and SecA recognize its side chain pointing toward the cytoplasm. During the simulations (Sim3 and Sim4), the epitope recognition site in Fab maintained a stable interaction with Arg351 (Figure 3A,B). To investigate the structural properties of the PGIRPG motif, we calculated the rmsd for this region. In Sim3, the average rmsd of the backbone atoms in the PGIRPG motif was <0.4 Å, indicating its structural rigidity in the Fab−ttSecYE form. Interestingly, the rmsd of the same region in Sim1 was also <0.4 Å, suggesting intrinsic rigidity. To examine the conformational properties of the PGIRPG motif, we compared the fluctuation of the backbone dihedral angle of Gly349 in this motif with that of Gly256 in the C4 loop. As shown in panels C and D of Figure 3, Gly349 is trapped at one of the conformational states of glycine while Gly256 fluctuates between multiple local minimum states. Other residues in the C4 and C5 loops also demonstrate a similar tendency (Figure S8 of the Supporting Information). The two proline residues, Pro348 and Pro353, likely restrict backbone dihedral angle rotation in the PGIRPG motif.

Because the Fab is not an actual channel partner, we investigated the structural properties of the PGIRPG motif making a model of SecA-bound SecYE in the pre-open form. Cross-linking experiments have indicated that the Leu775Cys mutation in ttSecA and the Pro352Cys mutation in the PGIRPG motif of ttSecY form a disulfide bond on oxidation (*14*). On the basis of this information, we docked ttSecA (PDB entry 2IPC) on ttSecYE in the pre-open form to create a Fab−ttSecYE-like structure and performed an all-atom MD simulation for 20 ns (Figure S9 of the Supporting Information). It was found that the interfacial region between ttSecA and ttSecY was similar to that of Fab-bound ttSecYE, and the fluctuations of the dihedral angles in the PGIRPG motif were suppressed as observed in Fab-bound ttSecYE. The conformation of ttSecYE hardly changed over the 20 ns MD simulation. The rigidity in the PGIRPG motif of SecY may facilitate binding of the channel partner and also be critical to the induced conformational change in TM8 and TM9.

Protein−*Lipid Interactions during the Conformational Transition of SecY*. To further investigate stabilization of the pre-open form of SecY, we analyzed the motion of lipid molecules near the hydrophobic crack region of SecY. In the starting structure of Sim1, no lipid molecule is located inside the

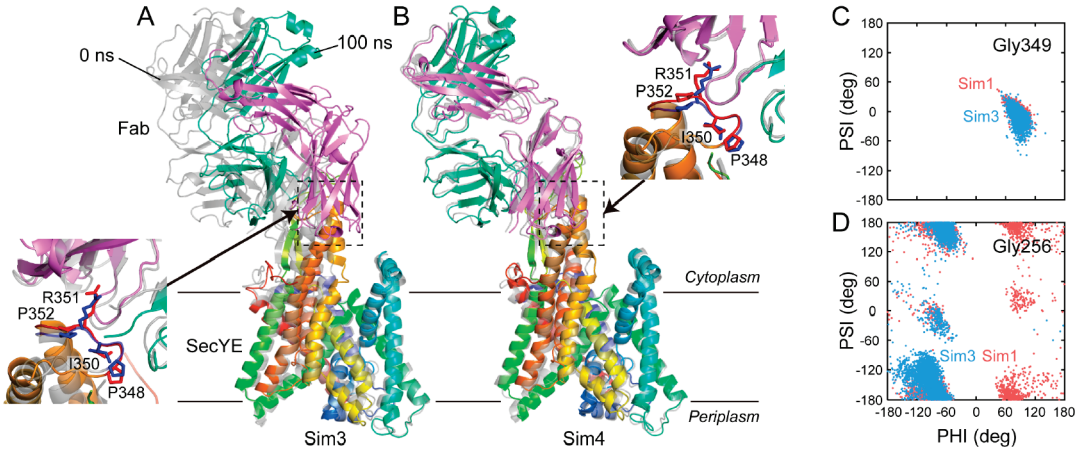

FIGURE 3: Effect of the binding of Fab on the conformational change of SecY. (A and B) Conformational change of Fab-bound ttSecYE in (A) Sim3 and (B) Sim4, in a comparison of the initial (0 ns, transparent gray) and final (100 ns, colored) structure. The structures are fitted to the Cα atoms of SecY. The inset is the interfacial region between Fab and the C5 loop of ttSecYE, where the structures are fitted to the Cα atoms of Fab. The PGIRPG motif presented in the stick model is colored blue (0 ns) and red (100 ns). (C and D) Fluctuations of the backbone dihedral angles of (C) Gly349 in the C5 loop and (D) Gly256 in the C4 loop, in a comparison of Sim1 and Sim3.

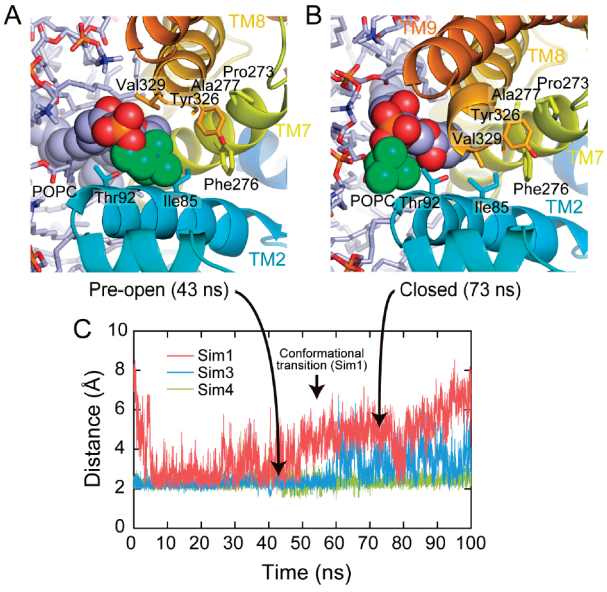

FIGURE 4: Lateral movement of the intercalated lipid molecule located in the hydrophobic crack. (A and B) Cytoplasmic view of the lateral gate region of SecY in Sim1. The intercalated lipid is outlined in the sphere model, where the green spheres represent the carbons of the choline group. The structure observed at 43 ns was defined as the pre-open form, in which the distance between Thr92 and Val329 was largest before the conformational transition occurred (see Figure S4B of the Supporting Information). The side chains of Thr92, Val329, and the highly conserved hydrophobic residues in the crack region are outlined in the stick model. (C) Time evolution of the minimum distance between the side chain atoms of Tyr326 and the intercalated lipid in Sim1, Sim3, and Sim4.

crack. However, one lipid near the lateral gate moves into the crack in the pre-open form (Figure 4A) and exits by a lateral movement when SecY adopts the closed form (Figure 4B). The intercalation of the lipid molecule is also observed in Sim3 and Sim4, although in the former the lipid also exits from the crack as observed in Sim1 while in the latter it stays for the entire 100 ns. To assess the movement of this lipid and the relationship with the conformational transition of SecY more quantitatively, we measured the distance between this lipid and Tyr326 in the hydrophobic crack (Figure 4C). In Sim1, Sim3, and Sim4, the distance approaches ~2 Å after 10 ns. In Sim1, the distance increases and largely fluctuates after 50 ns, indicating dissociation of the lipid headgroup from the hydrophobic crack. In Sim3, the distance also fluctuates after 60 ns, again showing the exit from the crack. In contrast, the distance during Sim4 remains unchanged. As shown in Figure 2A (Sim1), TM8 tilts toward TM2 and the hydrophobic crack is filled during the conformational transition of SecY. This conformational change occurs at 55 ns (Figure 1A, red line) and correlates with the increase and fluctuation of the distance between the lipid and Tyr326 (Figure 4C, red line). Thus, the lateral movement of the lipid molecule is synchronized with the conformational transition of SecY. We also performed a simulation for Fab-free ttSecYE in which the intercalated lipid was restrained to stay in the crack. Significantly, SecY remains in a pre-open form (Figure S10 of the Supporting Information). The changes in protein−lipid and intraprotein interactions are likely essential for the conformational transition of SecY, and in fact, the transition may be triggered by the lateral movement and intercalation of the lipid molecule. Because Tyr326 is the only polar residue among the highly conserved residues (Ile85, Pro273, Phe276, Ala277, and Tyr326) forming the hydrophobic crack (*14*), we considered whether there might be specific interactions between Tyr326 and the intercalated lipid. However, an analysis revealed no clear hydrogen bonding interactions between them, suggesting that the lipid may simply fill the crack or void. The inhibition of formation of the disulfide bond between Thr92(TM2) and Val329(TM8) under SecA-containing conditions (*14*) may be due to this intercalated lipid molecule.

The functional importance of protein−lipid interactions during translocation of protein through the Sec channel has been demonstrated in experimental and theoretical studies. The cross-linking experiments indicated that the signal sequence interacts not only with TM2 and TM7 helices but also with surrounding lipid molecules during protein translocation (*29*). The cross-linked lipid may correspond to our intercalated lipid. Gumbart and Schulten have performed simulations of the lateral gate opening of mjSecYEβ with strong artificial forces using the Steered MD method and observed the intercalation of one or two lipid molecules in the lateral gate region (*17*). They also suggested that the entry and exit of lipid molecules from the

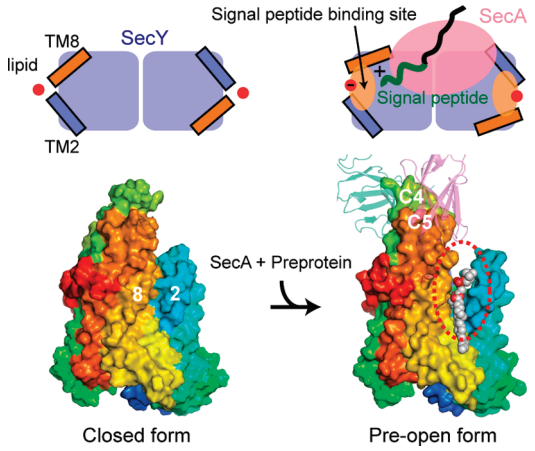

FIGURE 5: Proposed mechanism underlying the early stage of protein translocation through the SecY channel. In the top panel, the square and ellipsoid diagrams represent SecY and SecA, respectively, as viewed from the cytoplasm. One copy of SecY serves as a SecA-docking site, while the other functions as a translocation pore. The size and position of SecA relative to SecY are illustrated arbitrarily. The bottom panels shows the conformational transition of SecY from the closed to pre-open form. The intercalated lipid molecule observed in our simulation in the pre-open form is outlined in the sphere model. The hydrophobic crack is circled with a dotted ellipsoid.

lateral gate are related to the conformational changes of mjSecYEβ, which is similar to our proposal. However, we think that the putative role of the lipid, which we discuss in this work, is different from theirs: they discussed the role of such lipid in lateral gate opening of SecY, when SecY integrates a protein into membranes. We are proposing another role of a lipid molecule at the early stage of protein translocation through the SecY channel upon the channel-partner binding.

It is well-established that phosphatidylethanolamine (PE) and phosphatidylglycerol (PG) are the major plasma membrane components in *Escherichia coli* and that anionic phospholipids are necessary for protein secretion in vivo and in vitro (*30*). The negatively charged headgroup of lipids has been proposed to be important for effective interaction with the positively charged N-terminus of the translocating signal sequence (*31*, *32*). In our previous paper, substitution of the amino acid residues in the hydrophobic crack in the lateral gate abolished SecY activity (*14*), which suggested that the hydrophobic crack provides a binding site for the signal sequence. Together with the simulation results, the deleterious effect on activity may come from weaker hydrophobic interactions between SecY and the intercalated lipid. These suggestions lead to the hypothesis that the intercalated lipid molecule between TM2 and TM8 (hydrophobic crack) in the pre-open state of SecY may facilitate the swift intercalation of the signal sequence.

Molecular Mechanisms for the Early Stage of Protein Translocation. We proposed a mechanism for the conformational transition of SecY from closed to pre-open forms upon SecA binding in our previous paper (*14*). On the basis of the current MD simulations and recent experiments, we expand the mechanism indicating the role of the conformational change of SecY and protein−lipid interactions. Figure 5 shows the outline of the proposed mechanism for the early stage of protein translocation, where we adopt the back-to-back model for Sec dimerization (*33*, *34*). The closed form of SecY, with the plug helix centrally located in the channel and the lateral gate closed, is a dominant conformation under the SecA-free condition. SecA approaches and recognizes the highly conserved PGIRPG motif in the C5 loop of SecY. Binding changes the conformation of SecY and opens the hydrophobic crack between TM2 and TM8, without altering the position of the plug helix, to yield a pre-open form. The rigidity of the PGIRPG motif may be important to the induction of the conformational change in the transmembrane region of SecY. Our simulations clearly demonstrated that during the conformational transition, a lipid molecule near the lateral gate of SecY immediately intercalates into the hydrophobic crack by sideways movement to stabilize the pre-open form of SecY. The negatively charged phosphoryl portion of the lipid headgroup may also act to attract the positively charged N-terminus of the signal sequence (*31*, *32*) for initial entry of a translocating protein into the channel. We suggest that these dynamic interactions involving not only protein−protein but also protein−lipid interactions play key roles in SecY channel function.

CONCLUSIONS

In this work, we performed all-atom model MD simulations of the protein-conducting SecY channel in membranes to investigate molecular mechanisms underlying the conformational transition between closed and pre-open forms of SecY. The closed form of SecY is stable with hardly any structural changes occurring during simulation, and the pre-open form without the channel partner quickly reverts to the closed form. The binding of Fab suppresses this conformational change in SecY. Importantly, the conformational transition between pre-open and closed forms correlates with the lateral movement of a lipid molecule in and out of a hydrophobic crack. We suggest that the stabilization of the pre-open form of SecY is achieved by not only the channel-partner binding but also the intercalation of the phospholipid in the hydrophobic crack of SecY.

It should be pointed out, however, that the time scale of the full functional cycle for protein secretion is much longer than the current simulations and the mechanisms of interconversion between pre-open and SecA-bound forms remain unrevealed. Further crystal structures, biochemical experiments, as well as long time all-atom model or coarse-grained model MD simulations for the SecA−SecY complex and with other Sec family proteins will be required to reveal the molecular mechanism underlying later stages of translocation of protein through the Sec translocon.

ACKNOWLEDGMENT

We thank Hiroyuki Mori and Koreaki Ito of the Institute of Virus Research, University of Kyoto (Kyoto, Japan), for helpful discussions. We thank the RIKEN Super Combined Cluster (RSCC) and RIKEN Integrated Cluster of Clusters (RICC) for providing computational resources.

SUPPORTING INFORMATION AVAILABLE

Four movies of Sim1−Sim4, modeling of the protein−membrane structures, equilibration procedure of MD simulations, and additional analysis of the MD trajectories. This material is available free of charge via the Internet at http://pubs.acs.org.

REFERENCES

1. Van den Berg, B., Clemons, W. M., Jr., Collinson, I., Modis, Y., Hartmann, E., Harrison, S. C., and Rapoport, T. A. (2004) X-ray structure of a protein-conducting channel. *Nature 427*, 36–44.

2. Rapoport, T. A. (2007) Protein translocation across the eukaryotic endoplasmic reticulum and bacterial plasma membranes. *Nature 450*, 663–669.
3. Mitra, K., Schaffitzel, C., Shaikh, T., Tama, F., Jenni, S., Brooks, C. L., III, Ban, N., and Frank, J. (2005) Structure of the *E. coli* protein-conducting channel bound to a translating ribosome. *Nature 438*, 318–324.
4. Menetret, J. F., Schaletzky, J., Clemons, W. M., Jr., Osborne, A. R., Skanland, S. S., Denison, C., Gygi, S. P., Kirkpatrick, D. S., Park, E., Ludtke, S. J., Rapoport, T. A., and Akey, C. W. (2007) Ribosome binding of a single copy of the SecY complex: Implications for protein translocation. *Mol. Cell 28*, 1083–1092.
5. Douville, K., Price, A., Eichler, J., Economou, A., and Wickner, W. (1995) SecYEG and SecA are the stoichiometric components of preprotein translocase. *J. Biol. Chem. 270*, 20106–20111.
6. Hunt, J. F., Weinkauf, S., Henry, L., Fak, J. J., McNicholas, P., Oliver, D. B., and Deisenhofer, J. (2002) Nucleotide control of interdomain interactions in the conformational reaction cycle of SecA. *Science 297*, 2018–2026.
7. Osborne, A. R., Clemons, W. M., Jr., and Rapoport, T. A. (2004) A large conformational change of the translocation ATPase SecA. *Proc. Natl. Acad. Sci. U.S.A. 101*, 10937–10942.
8. Vrontou, E., and Economou, A. (2004) Structure and function of SecA, the preprotein translocase nanomotor. *Biochim. Biophys. Acta 1694*, 67–80.
9. Mori, H., and Ito, K. (2001) The Sec protein-translocation pathway. *Trends Microbiol. 9*, 494–500.
10. Veenendaal, A. K., van der Does, C., and Driessen, A. J. (2004) The protein-conducting channel SecYEG. *Biochim. Biophys. Acta 1694*, 81–95.
11. Papanikou, E., Karamanou, S., and Economou, A. (2007) Bacterial protein secretion through the translocase nanomachine. *Nat. Rev. Microbiol. 5*, 839–851.
12. Li, W., Schulman, S., Boyd, D., Erlandson, K., Beckwith, J., and Rapoport, T. A. (2007) The plug domain of the SecY protein stabilizes the closed state of the translocation channel and maintains a membrane seal. *Mol. Cell 26*, 511–521.
13. Zimmer, J., Nam, Y., and Rapoport, T. A. (2008) Structure of a complex of the ATPase SecA and the protein-translocation channel. *Nature 455*, 936–943.
14. Tsukazaki, T., Mori, H., Fukai, S., Ishitani, R., Mori, T., Dohmae, N., Perederina, A., Sugita, Y., Vassylyev, D. G., Ito, K., and Nureki, O. (2008) Conformational transition of Sec machinery inferred from bacterial SecYE structures. *Nature 455*, 988–991.
15. Haider, S., Hall, B. A., and Sansom, M. S. (2006) Simulations of a protein translocation pore: SecY. *Biochemistry 45*, 13018–13024.
16. Tian, P., and Andricioaei, I. (2006) Size, motion, and function of the SecY translocon revealed by molecular dynamics simulations with virtual probes. *Biophys. J. 90*, 2718–2730.
17. Gumbart, J., and Schulten, K. (2007) Structural determinants of lateral gate opening in the protein translocon. *Biochemistry 46*, 11147–11157.
18. Tam, P. C., Maillard, A. P., Chan, K. K., and Duong, F. (2005) Investigating the SecY plug movement at the SecYEG translocation channel. *EMBO J. 24*, 3380–3388.
19. Kale, L., Skeel, R., Bhandarkar, M., Brunner, R., Gursoy, A., Krawetz, N., Phillips, J., Shinozaki, A., Varadarajan, K., and Schulten, K. (1999) NAMD2: Greater scalability for parallel molecular dynamics. *J. Comput. Phys. 151*, 283–312.
20. MacKerell, A. D., Jr., Bashford, D., Bellott, M., Dunbrack, R. L., Jr., Evanseck, J. D., Field, M. J., Fischer, S., Gao, J., Guo, H., Ha, S., Joseph-McCarthy, D., Kuchnir, L., Kuczera, K., Lau, F. T. K., Mattos, C., Michnick, S., Ngo, T., Nguyen, D. T., Prodhom, B., Reiher, W. E., III, Roux, B., Schlenkrich, M., Smith, J. C., Stote, R., Straub, J., Watanabe, M., Wiorkiewicz-Kuczera, J., Yin, D., and Karplus, M. (1998) All-atom empirical potential for molecular modeling and dynamics studies of proteins. *J. Phys. Chem. B 102*, 3586–3616.
21. Mackerell, A. D., Jr., Feig, M., and Brooks, C. L., III (2004) Extending the treatment of backbone energetics in protein force fields: Limitations of gas-phase quantum mechanics in reproducing protein conformational distributions in molecular dynamics simulations. *J. Comput. Chem. 25*, 1400–1415.
22. Darden, T., York, D., and Pedersen, L. (1993) Particle mesh Ewald: An N.log(N) method for Ewald sums in large systems. *J. Chem. Phys. 98*, 10089–10092.
23. Hubbard, S. J., and Thornton, J. M. (1993) NACCESS, Department of Biochemistry and Molecular Biology, University College London, London.
24. Petrek, M., Kosinova, P., Koca, J., and Otyepka, M. (2007) MOLE: A Voronoi diagram-based explorer of molecular channels, pores, and tunnels. *Structure 15*, 1357–1363.
25. Hayward, S., Kitao, A., and Berendsen, H. J. (1997) Model-free methods of analyzing domain motions in proteins from simulation: a comparison of normal mode analysis and molecular dynamics simulation of lysozyme. *Proteins 27*, 425–437.
26. Mori, H., and Ito, K. (2001) An essential amino acid residue in the protein translocation channel revealed by targeted random mutagenesis of SecY. *Proc. Natl. Acad. Sci. U.S.A. 98*, 5128–5133.
27. de Keyzer, J., Regeling, A., and Driessen, A. J. (2007) Arginine 357 of SecY is needed for SecA-dependent initiation of preprotein translocation. *FEBS Lett. 581*, 1859–1864.
28. Cheng, Z., Jiang, Y., Mandon, E. C., and Gilmore, R. (2005) Identification of cytoplasmic residues of Sec61p involved in ribosome binding and cotranslational translocation. *J. Cell Biol. 168*, 67–77.
29. Plath, K., Mothes, W., Wilkinson, B. M., Stirling, C. J., and Rapoport, T. A. (1998) Signal sequence recognition in posttranslational protein transport across the yeast ER membrane. *Cell 94*, 795–807.
30. van Dalen, A., and de Kruijff, B. (2004) The role of lipids in membrane insertion and translocation of bacterial proteins. *Biochim. Biophys. Acta 1694*, 97–109.
31. McKnight, C. J., Briggs, M. S., and Gierasch, L. M. (1989) Functional and nonfunctional LamB signal sequences can be distinguished by their biophysical properties. *J. Biol. Chem. 264*, 17293–17297.
32. Keller, R. C., Killian, J. A., and de Kruijff, B. (1992) Anionic phospholipids are essential for α-helix formation of the signal peptide of prePhoE upon interaction with phospholipid vesicles. *Biochemistry 31*, 1672–1677.
33. Breyton, C., Haase, W., Rapoport, T. A., Kuhlbrandt, W., and Collinson, I. (2002) Three-dimensional structure of the bacterial protein-translocation complex SecYEG. *Nature 418*, 662–665.
34. Osborne, A. R., and Rapoport, T. A. (2007) Protein translocation is mediated by oligomers of the SecY complex with one SecY copy forming the channel. *Cell 129*, 97–110.